Parkinsonism and Related Disorders 94 (2022) 30–36

Contents lists available at ScienceDirect

Parkinsonism and Related Disorders

journal homepage: www.elsevier.com/locate/parkreldis

Somatotopy of cervical dystonia in motor-cerebellar networks: Evidence from resting state fMRI

Giuseppe A. Zito [a], Clément Tarrano [a,b], Prasanthi Jegatheesan [a], Asya Ekmen [a], Benoît Béranger [c], Michael Rebsamen [d], Cécile Hubsch [e], Sophie Sangla [e], Cécilia Bonnet [a], Cécile Delorme [a,b], Aurélie Méneret [a,b], Bertrand Degos [f,g], Floriane Bouquet [b], Marion Apoil Brissard [h], Marie Vidailhet [a,b], Cécile Gallea [a,1], Emmanuel Roze [a,b,1,*], Yulia Worbe [a,i,1]

[a] Sorbonne University, Inserm U1127, CNRS UMR7225, UM75, Paris Brain Institute, Movement Investigation and Therapeutics Team, 47-83 Boulevard de l'Hôpital, 75013, Paris, France
[b] Department of Neurology, Assistance Publique-Hôpitaux de Paris, Pitié-Salpêtrière Hospital, 47-83 Boulevard de l'Hôpital, 75013, Paris, France
[c] Center for NeuroImaging Research CENIR, Paris Brain Institute, Sorbonne University, UPMC Univ Paris 06, Inserm U1127, CNRS UMR 7225, 47-83 Boulevard de l'Hôpital, 75013, Paris, France
[d] Support Center for Advanced Neuroimaging SCAN, University Institute of Diagnostic and Interventional Neuroradiology, Inselspital, Bern University Hospital, University of Bern, Freiburgstrasse, 3010, Bern, CH, Switzerland
[e] Department of Neurology, Rothschild Foundation, 25-29 Rue Manin, 75019, Paris, France
[f] Neurology Unit, Assistance Publique-Hôpitaux de Paris, Avicenne University Hospital, Sorbonne Paris Nord, 125 Rue de Stalingrad, 93000, Bobigny, France
[g] Center for Interdisciplinary Research in Biology, Collège de France, Inserm U1050, CNRS UMR 7241, PSL University, 11 place Marcelin Berthelot, 75231, Paris, France
[h] Department of Neurology, University of Caen Normandie Hospital Center, Av. de la Côte de Nacre, 14000, Caen, France
[i] Department of Neurophysiology, Saint-Antoine Hospital, Assistance Publique-Hôpitaux de Paris, 184 Rue du Faubourg Saint-Antoine, 75012, Paris, France

ARTICLE INFO

Keywords:
Cervical dystonia
Resting state fMRI
Motor cortex
Cerebellum

ABSTRACT

Introduction: Cervical dystonia is the most frequent form of isolated focal dystonia. It is often associated with a dysfunction in brain networks, mostly affecting the basal ganglia, the cerebellum, and the somatosensory cortex. However, it is unclear if such a dysfunction is somato-specific to the brain areas containing the representation of the affected body part, and may thereby account for the focal expression of cervical dystonia.
In this study, we investigated resting state functional connectivity in the areas within the motor cortex and the cerebellum containing affected and non-affected body representations in cervical dystonia patients.
Methods: Eighteen patients affected by cervical dystonia and 21 healthy controls had resting state fMRI. The functional connectivity between the motor cortex and the cerebellum, as well as their corresponding measures of gray matter volume and cortical thickness, were compared between groups. We performed seed-based analyses, selecting the different body representation areas in the precentral gyrus as seed regions, and all cerebellar areas as target regions.
Results: Compared to controls, patients exhibited increased functional connectivity between the bilateral trunk representation area of the motor cortex and the cerebellar vermis 6 and 7b, respectively. These functional abnormalities did not correlate with structural changes or symptom severity.

* Corresponding author. Salpêtrière Hospital, 47-83 Boulevard de l'Hôpital, 75013 Paris, France.
E-mail addresses: giuseppeangelo.zito@hest.ethz.ch (G.A. Zito), clement.tarrano@gmail.com (C. Tarrano), prasanthi.jegatheesan@aphp.fr (P. Jegatheesan), ekmenasya@gmail.com (A. Ekmen), benoit.beranger@icm-institute.org (B. Béranger), michael.rebsamen@students.unibe.ch (M. Rebsamen), c.hubsch@hotmail.fr (C. Hubsch), sophiesangla@orange.fr (S. Sangla), bonnet.cecilia@gmail.com (C. Bonnet), cecile.delorme@aphp.fr (C. Delorme), aurelie.meneret@aphp.fr (A. Méneret), bertrand.degos@aphp.fr (B. Degos), bouquetfloriane@gmail.com (F. Bouquet), apoil.marion@gmail.com (M.A. Brissard), marietoulousaine@gmail.com (M. Vidailhet), cecile.gallea.icm@gmail.com (C. Gallea), emmanuel.flamand-roze@aphp.fr (E. Roze), yworbe@gmail.com (Y. Worbe).
[1] These authors contributed equally to the work.

https://doi.org/10.1016/j.parkreldis.2021.11.034
Received 7 September 2021; Received in revised form 25 November 2021; Accepted 29 November 2021
Available online 30 November 2021

Conclusions: Our findings indicate that the abnormal function of the motor network is somato-specific to the areas encompassing the neck representation. Functional abnormalities in discrete relevant areas of the motor network could thus contribute to the focal expression of CD.

1. Introduction

Cervical dystonia (CD) is the most common form of isolated focal dystonia, characterized by involuntary muscle contractions in the neck, which results in abnormal head posture and movements [1]. It has been associated with various brain dysfunctions, such as maladaptive neuroplasticity, abnormal sensorimotor processing and integration [2], but its pathogenesis is still unclear [3].

CD is considered a network disorder arising from abnormal communication among different brain areas [2]. Neuroimaging studies have evidenced functional and structural abnormalities in the basal ganglia [2,4], the sensorimotor and frontoparietal regions, the insula, the cerebellum, and the brainstem [3,4]. Research indicates that both the cerebello-thalamo-cortical network and basal ganglia–thalamo--cortical network project into the motor cortex, where the motor output is generated, and may contribute to the abnormal movements [5]. Other studies focusing on the cerebellum have reported increased gray matter (GM) volume of cerebellar flocculus, in CD patients compared to healthy controls (HC) [6]. Altogether, these findings point to the motor cortex and the cerebellum as critical structures for the pathogenesis of CD.

It is mostly unknown whether these network abnormalities represent a general marker of the dystonia pathogenesis, irrespectively of the affected body part, or if the pathogenesis of different types of dystonia affects relevant discrete areas within the motor areas and cerebellum. Distinct patterns of altered microstructures within regions of basal ganglia and cerebellar circuits have been associated with different phenotypes of focal dystonia [7], and regional patterns of functional connectivity within the striatum. So far, there is no detailed study of the cerebellar somatotopy in CD, since a high-definition functional cerebellar atlas has been developed only recently [8]. Such an investigation is not trivial, as it has been shown that the representations of multiple body parts are organized in an orderly manner in the cerebellar lobes, mirroring the functional specialization of the motor cortex [8].

In this study, we investigated the specificity of motor-cerebellar networks in CD using resting state functional connectivity (RS-FC). RS-FC is a widely used non-invasive technique, based on functional magnetic resonance imaging (fMRI), where the time courses of the BOLD signal in predefined regions of interest (ROIs) are extracted from the brain at rest, and correlated with each other, under the assumption that functionally connected areas show high correlation [9]. We compared patterns of RS-FC in the different body representation areas of the motor cortex and the cerebellum between patients affected by CD and HC, and performed a morphometric analysis on the same areas to study differences in GM volumes and cortical thickness (CT) between groups. We tested the hypothesis that network dysfunctions in CD are somato-specific, i.e., CD patients exhibit abnormal RS-FC and structural differences only in the head and neck representation areas, in both the motor cortex and the cerebellum.

2. Materials and methods

2.1. Subjects and general procedure

We recruited 18 CD patients (7 males, mean age = 46.9 ± 8.7 years) and 21 sex- and age-matched HC (9 male, mean age = 45.3 ± 10.6 years). Patients were recruited at the Pitié-Salpêtrière Hospital, Paris, FR. Inclusion criteria for patients were: a clinical diagnosis of idiopathic CD, no botulinum toxin injection within 3 months prior to the examination, and stable pharmacological treatment in the month preceding inclusion. Exclusion criteria common to both HC and CD patients were: i) any other neurological sign or dystonia in other body parts, ii) incompatibility with MR acquisition, and iii) secondary aetiologies (such as exposure to the dopamine receptors blockers, focal brain lesions) of CD as evaluated by considering the medical history. Of note, the patients had no genetic analysis. Patients with severe symptoms or tremor were excluded to ensure good image quality. Severity of CD was assessed at the time of inclusion with the Toronto Western Spasmodic Torticollis Rating Scale (TWSTRS), subscale for severity [10]. Between-group differences in age were assessed with independent-sample t-tests, whereas differences in the ratio between male and female participants were assessed with χ^2 tests.

The study was carried out in accordance with the latest version of the Declaration of Helsinki and approved by the local Ethics Committee (approval number: C17-04 - AU 1360, ClinicalTrial.gov ID: NCT03351218). All participants gave written informed consent prior to the study.

2.2. Neuroimaging acquisition parameters and pre-processing

During the MR session, participants lied in the scanner while fixating a cross displayed on a screen. Their gaze was monitored with eye-tracking. Neuroimaging data were acquired using a 3T Magnetom Prisma (Siemens, DE) with a 64-channel head coil. Resting state fMRI and structural images were acquired in one session. Structural images were acquired with a T1-weighted MP2RAGE sequence with Repetition Time (TR) = 5 s, Inversion Time (TI) = 700/2500 ms, field of view (FOV) = 232 × 256 in plane × 176 slices, 1 mm isotropic, Ipat acceleration factor = 3. FMRI data were acquired with an echo-planar imaging (EPI) sequence performed with a multi-slice, multi-echo acquisition, TR = 1.9 s, Echo Time (TE) = 17.2/36.62/56.04 ms, Ipat acceleration factor = 2, Multi-band = 2, isotropic voxel size = 3 mm, dimensions = 66 × 66 in plane × 46 slices, 350 vol, duration = 11 min. The scan duration was chosen based on reliability measures of RS-FC data [11,12], and on evidence of no significant gains over 12 min of acquisition [13].

Image preprocessing was done as follows: structural images were background denoised in order to improve the quality of the subsequent steps, segmented and normalized to the Montreal Neurological Institute (MNI) space using the Computational Anatomy Toolbox (CAT12 - http://www.neuro.uni-jena.de/cat/) extension for SPM12 (https://www.fil.ion.ucl.ac.uk/spm/software/spm12/). Among the various methods for pre-processing and analysis of fMRI studies [14], we employed a pre-processing strategy which, although very conservative, has proven to be robust in denoising RS-FC data, especially those induced by head movements artefacts [15–18]. Functional images were first pre-processed according to standard pipelines, i.e., despiking, slice timing correction and realignment using AFNI (https://afni.nimh.nih.gov/). For the latter step, the parameters for motion correction were estimated from the first echo, and applied to all other echoes. A brain mask was computed on the realigned shortest echo temporal mean using FSL BET [19] in order to increase the robustness against signal bias intensity. Afterwards, the TEDANA toolbox [20] version 0.0.7 was used to optimally combine the realigned echoes, to apply principal component analysis and reduce the dimensionality of the data, and to perform an independent component analysis (ICA) decomposition to separate BOLD and non-BOLD components [20]. This step ensured robust artefact removal of non-BOLD signals, such as movement, respiration or heartbeat, and has already shown to be superior over standard denoising techniques in regressing out motion [21,22]. In order to verify the quality of the pre-processing, we calculated the temporal standard

deviation (tSTD) of the raw data, after the first pre-processing steps (despiking, slice timing correction and realignment), of the optimally combined data, and after denoise with ICA. We verified that tSTD decreased at each step of the pre-processing, and it never differed between CD patients and HC (Supplementary Material and Supplementary Fig. 1). Framewise displacement (FD) was further computed according to standard methods [23], and compared between CD patients and HC. The quality of the signal was verified as head movement amplitude was minimal, the FD of the raw data, as well as the one of the pre-processed data, never exceeded the threshold of 0.5 mm recommended for motion scrubbing [24], and it did not statistically differ between CD patients and HC ($p > 0.050$, details as Supplementary Material and Supplementary Fig. 2 [25]). We thus retained all 350 vol for further analyses. Finally, using SPM12, functional images were co-registered to the T1-weighted image, normalized to MNI space, and smoothed with a Gaussian kernel with full width at half maximum of 4 × 4x4 mm, as previously suggested [26].

After pre-processing, the CONN toolbox [27] implemented in Matlab r2018a (The MathWorks Inc. USA) was used to parcellate the brain images into 274 functional regions, based on the Brainnetome Atlas [26], and to extract the region-averaged time series. Motion parameters obtained during the realignment, as well as the average signal of white matter and cerebrospinal fluid obtained during the segmentation, were regressed out with aCompCor [28]. This step reduced spatial correlations resulting from physiological noise. Time series were finally band-pass filtered at $0.01 < f < 0.1$ Hz, according to previous research [26].

2.3. Analysis of resting state functional connectivity

We entered all the time series extracted from the 274 functional regions into a first level general linear model (GLM), where we performed a ROI-based analysis, for each participant, to determine significant resting state connections at individual level: In particular, we used bivariate correlation coefficients between all pairs of ROIs as indicators of their functional connectivity. False discovery rate (FDR) with a threshold of $p_{FDR}<0.050$ was implemented to correct for multiple comparisons. Next, we converted the correlation coefficients to z-scores using Fisher-z transformation, in order to normalize them to a Gaussian distribution. We then implemented a second level GLM testing seed-based ROI-to-ROI differences between CD and HC. For the latter, as we were only interested in the connectivity between the motor cortex and the cerebellum, we isolated the regions of the Brainnetome Atlas that were associated with the body representation areas within the precentral gyrus (PrG) and paracentral lobule (PCL), as well as all cerebellar regions without a priori, i.e. irrespective of body representation (Table 1). We then selected the bilateral motor areas as seed ROIs and the cerebellar ROIs as target regions. False positive control for multiple comparisons was implemented using false FDR-corrected p-values with a threshold of $p_{FDR}<0.050$.

A correlation analysis was performed by computing Pearson correlation's coefficients between the severity of dystonia (TWSTRS scores) and the connectivity values between the motor cortex and the cerebellum. A FDR-corrected threshold of $p_{FDR}<0.050$ was applied.

2.4. Analysis of structural data

We performed a morphometric analysis to study differences in GM volume between CD patients and HC. After preprocessing, the normalized GM volumes obtained during the segmentation were smoothed using a 4 mm full breadth at half maximum kernel, in line with our functional analysis. Volumes from the ROIs in the motor cortex were extracted with CAT12 using the "ROI tool" option, whereas volumes in the cerebellar ROIs were extracted with the Spatially Unbiased Infratentorial toolbox (SUIT) [29]. For the latter, we first isolated the infratentorial structures using *suit_isolate_seg*, we then performed an affine alignment to the specific SUIT template and applied a normalisation using *suit_normalize_dartel*, and finally we extracted the GM volumes using *suit_reslice_dartel*.

We also studied differences in CT between patients and controls, by extracting CT in the investigated ROIs with DL + DiReCT [30]. This method already showed high accuracy compared to standard instruments [30]. Due to the lack of available tools to reliably measure CT in the cerebellum, this analysis was performed only for the somatotopic regions of the motor cortex.

The extracted GM volumes and CTs were compared between groups with independent-sample t-tests implemented in SPSS 25 (IBM Inc., USA). A threshold of $p < 0.050$ was selected.

Table 1
List of seed and target ROIs used in the analysis of functional connectivity. The Brainnetome Atlas was used to isolate all regions associated with the body representation areas within the motor cortex, as well as all cerebellar regions. R = right, L = left, PrG = precentral gyrus. PCL = paracentral lobule.

Seed regions (Motor cortex)	MNI coordinates (x, y,z)	Target regions (Cerebellum)	MNI coordinates (x, y,z)
R/L PrG, area 4 (head and face region)	R: 55, −2, 33 L: −49, −8, 39	R/L Lobules 1, 2, 3, 4	R: 10–43 -18 L: 7 -44 -17
R/L PrG, area 6 (caudal dorsolateral region)	R: 33, −7, 57 L: −32, −9, 58	R/L Lobule 5	R: 14–51 -19 L: 13 -50 -19
R/L PrG, area 4 (upper limb region)	R: 34, −19, 59 L: −26, −25, 63	R/L Lobule 6	R: 24–58 -25 L: 23 -59 -25
R/L PrG, area 4 (trunk region, including neck)	R: 15, −22, 71 L: 15, −22, 71	R/L Lobule 7b	R: 28–66 -51 L: 26 -66 -51
R/L PrG, area 4 (tongue and larynx region)	R: 54, 4, 9 L: −52, 0, 8	R/L Lobule 8a	R: 26–58 -53 L: 24 -57 -53
R/L PrG, area 6 (caudal ventrolateral region)	R: 51, 7, 30 L: −49, 5, 30	R/L Lobule 8b	R: 18–51 -55 L: 17 -50 -55
R/L PCL, areas 1, 2, 3 (lower limb region)	R: 10, −34, 54 L: −8, −38, 58	R/L Lobule 9	R: 7–53 -49 L: 7 -53 -48
R/L PCL, area 4 (lower limb region)	R: 5, −21, 61 L: −4, −23, 61	R/L Lobule 10	R: 22–37 -46 L: 21 -37 -45
		R/L Crus 1	R: 38–68 -32 L: 36 -68 -32
		R/L Crus 2	R: 26–76 -41 L: 26 -75 -42
		Vermis 6	1 -70 -21
		Vermis/Crus 1	−4 -78 -27
		Vermis/Crus 2	1 -75 -31
		Vermis 7b	0 -68 -31
		Vermis 8a	0 -67 -38
		Vermis 8b	0 -63 -42
		Vermis 9	0 -56 -37
		Vermis 10	1 -48 -35

3. Results

No significant differences were found in age and sex ratio between male and female participants (Table 2). CD patients showed symptom severity of 18.3 ± 4.4, as assessed with the TWSTRS.

3.1. Resting state functional connectivity and structural analysis

The analysis of RS-FC revealed increased functional connectivity, in CD patients compared to HC, of the bilateral trunk representation area 4 (PrG) with the cerebellar Vermis 6 [$F(2,36) = 10.78$, $p_{FDR} = 0.039$] and Vermis 7b [$F(2,36) = 10.33$, $p_{FDR} = 0.039$], respectively. Detailed values of RS-FC, as well as the functional connectivity maps in the two groups, are displayed in Fig. 1 and Fig. 2, respectively. No significant differences in the connectivity between the other seed ROIs and the cerebellum (Table 1) were found across groups ($p_{FDR}>0.050$ – Supplementary Fig. 3).

No correlation was found between any of the investigated connections and symptoms' severity in CD ($p_{FDR}>0.050$ – Supplementary

Table 2
Clinical and demographic information. Comparison of clinical and demographic scores between groups. TWSTRS = Toronto Western Spasmodic Torticollis Rating Scale, HC = healthy controls, CD = cervical dystonia, BoT = botulinum toxin.

	HC (N = 21)	CD (N = 18)	Statistics
Sex [male/female]	9/12	7/11	$\chi(1) = 0.06$, $p = 0.802$
Age [years, mean ± SD]	45.3 ± 10.6	46.9 ± 8.7	$t(37) = 0.53$, $p = 0.600$
TWSTRS	–	18.3 ± 4.4	–
Overall medication [N (% of CD)]	–	18 (100%)	
- BoT [N (% of TD)][a]	–	17 (94.4%)	
- Others (Tramadol, Levothyroxine, Diazepam, Escitalopram – [N (% of CD)])	–	3 (16.7%)	

[a] Last BoT injection administered at least 3 months prior to the experiment.

Fig. 4). Neither differences in GM volume, nor in CT, were found between the studied groups, in any of the investigated ROIs ($p > 0.050$).

4. Discussion

Compared to HC, patients with CD showed increased functional connectivity between the neck and trunk representation in area 4 of the precentral gyrus (PrG) and the cerebellar Vermis 6 and 7b. This pattern was neither associated with differences in GM volumes or CT between groups, nor with symptoms' severity in CD. Our findings indicate that the abnormal function of the motor network is somato-specific to the areas encompassing the neck and trunk representation. Functional abnormalities in discrete relevant areas of the motor network could thus relate to the focal expression of CD.

The use of resting state fMRI was a strength of this study, as it allowed us to investigate task-free patterns of functional connectivity, hence, to avoid a potential bias due to adaptive/compensatory processes associated with task execution. This is relevant, as dystonic symptoms tend to worsen during voluntary motor activity, and compensatory mechanisms are more likely to occur during task execution than rest [31]. However, neuroimaging analyses can hardly distinguish causes from effects. Even though our results are consistent with previous findings on CD pathogenesis, the causal mechanisms here discussed are speculative.

One limitation of the current study is the relatively small sample size. We chose to recruit 39 participants based on existing literature on resting state fMRI in CD [31–34], as current tools for power analysis have been deemed as unreliable when applied to neuroimaging data [35]. However, our sample may not be representative of the entire population.

The study of the somatotopy in dystonia has shown controversial results. For instance, previous studies have identified aberrant somatotopic representations in the primary motor and somatosensory cortices, as well as the cerebellum, in various forms of dystonia, and hypothesized that maladaptive plasticity likely corresponds to a disorganized somatotopy in dystonia [36–38]. However, specific somatotopic representations in motor-related areas were not associated to the dystonic symptoms [36].

The cerebellum is of particular importance for the pathophysiology of CD, as the topographical expression of dystonia depends on the extent of cerebellar dysfunction in a dedicated mouse model [39]. In this model, a dysfunction of the entire cerebellum induces a phenotype similar to generalized dystonia, whereas dysfunctions in limited cerebellar regions restrict abnormal movements to isolated body parts, like in focal dystonia. Hence, the extent, but not the location of the cerebellar dysfunction, seems to be linked to the severity of dystonia. Altered connectivity between the cerebellum and the sensorimotor areas has also been associated with the pathogenesis of CD [3]. However, reported changes were not limited to the somatotopic representation of the affected body parts [3], and the potential link between critical areas within these regions and the location of dystonic manifestations is still poorly understood. Our results challenge this view, and provide evidence of well-defined regions in both the precentral gyrus (PrG) and the cerebellum specifically relevant to the clinical expression of CD, namely the trunk representation area 4 of the PrG and the cerebellar Vermis 6 and 7b. No other areas within the PrG and the cerebellum showed any group differences in RS-FC between patients and HC, thereby reinforcing the hypothesis of a selective area, with a critical role in motor control of head and neck, implicated in the pathogenesis of CD. More specifically, the trunk representation area 4 of the PrG contains neuronal populations responsible for motor control of the sternocleidomastoid muscle [40], typically affected in CD. Likewise, the cerebellar Vermis 6 has been related to saccadic eye movements in healthy subjects [41], and clinical studies have confirmed a link between abnormal cerebellar output and an impairment in saccadic adaptation in CD [42]. This may reflect cerebellar-related maladaptive plasticity associated with an attempt to compensate the abnormal head posture with a modulation of eye movements [43].

Abnormal connectivity of brain networks linking the cerebellum and the motor cortex has been largely investigated for its role in the pathogenesis of dystonia [4]. For instance, in mice [39], dystonic movements can be provoked by manipulations of the cerebellum, and in humans, abnormal anatomical cerebello-thalamo-cortical connectivity can play a role in the clinical expression of dystonia [44]. CD patients with a sensory trick show a differential ability to modulate the connectivity of the sensorimotor network, likely through a cerebellar mediation [33]. We hypothesize that the abnormal connectivity between the motor cortex and the cerebellum found in our study reflects a cerebellar dysfunction mediating sensorimotor integration and maladaptive plasticity. This interpretation is consistent with the head neural integrator model, by which changes in any of the inputs of the integrator affect the communication between the cerebellum and cortical areas, and potentially lead to the manifestation of CD [45]. In healthy subjects, proprioceptive

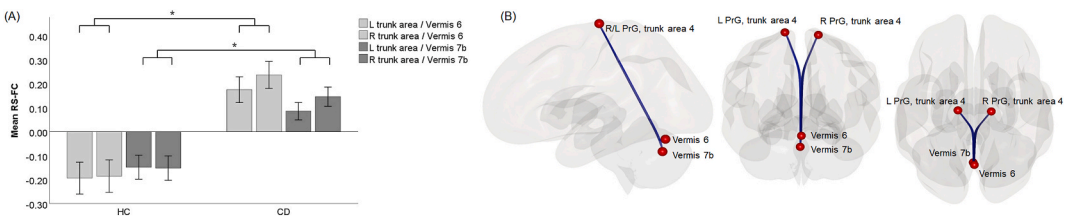

Fig. 1. Mean values of resting state functional connectivity, as represented by the Pearson correlation coefficients, between the seed ROIs in the precentral gyrus and the target ROIs in the cerebellum, separately for CD patients and HC. (A) Results of the general linear model. (B) Visual representation of the significant seeds and target ROIs. Error bars represent the standard error of the mean. * depicts significant differences ($p_{FDR}<0.050$) between CD patients and HC. (For interpretation of the references to color in this figure legend, the reader is referred to the Web version of this article.)

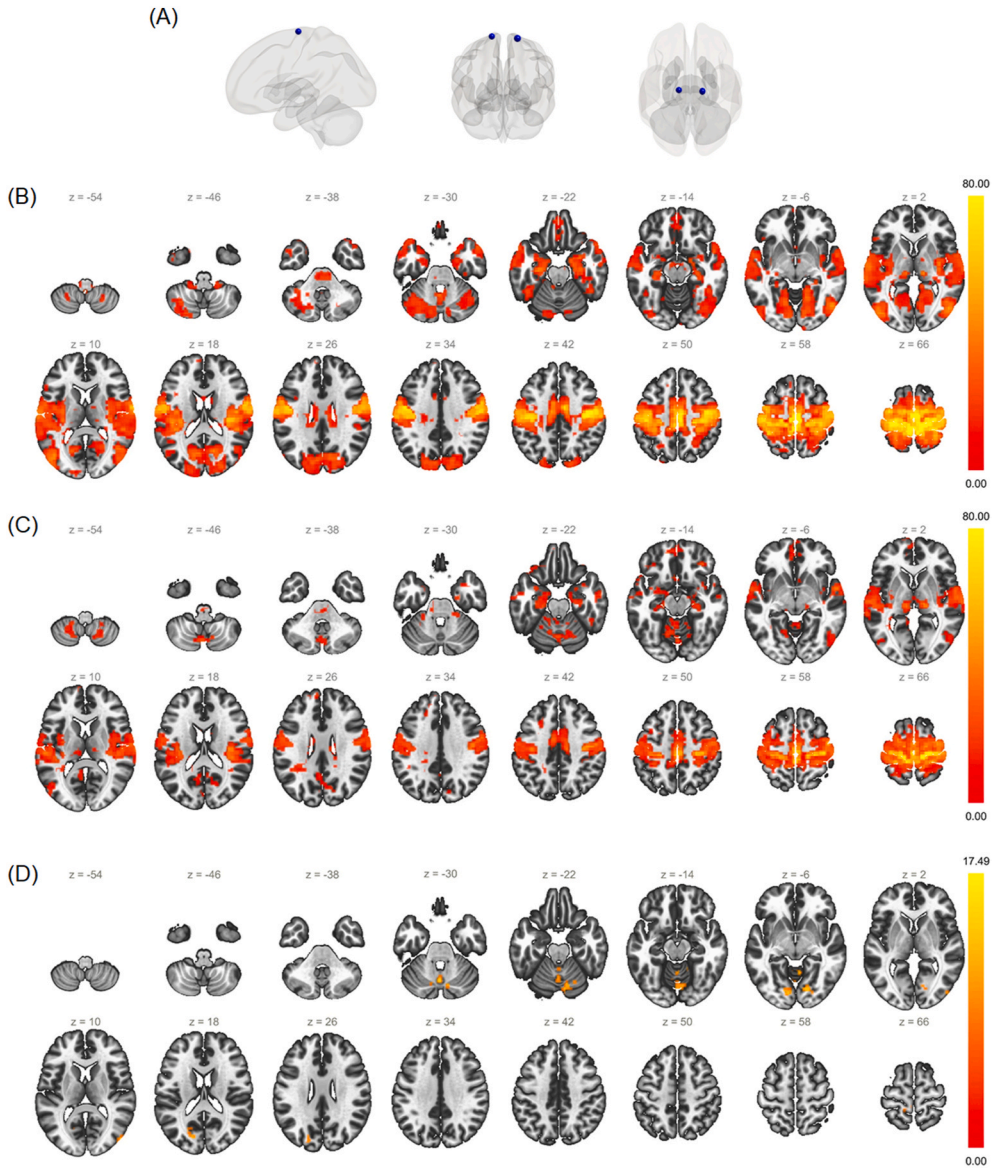

Fig. 2. Functional connectivity (FC) maps in the investigated groups. (A) Seed regions in the trunk representation area 4 of the PrG. (B) FC maps in HC. (C) FC maps in CD. (D) Difference in FC maps between HC and CD. Color bars represent the F values. (For interpretation of the references to color in this figure legend, the reader is referred to the Web version of this article.)

input from the neck can substantially change the way cerebellar output influences plasticity at the level of the motor cortex [46]. In CD, an abnormal integration of the neck proprioceptive information could drive an anomalous functioning of the integrator [46], which may generate an atypical head posture. The specific involvement of Vermis 6 and 7b found in our study provides further insights into the role of cerebellar areas associated with saccadic eye movements in the integrator dysfunction of CD [6].

The investigated differences in functional connectivity were not associated with structural changes in CD, as evidenced by our analysis of GM volume and CT, and this supports the concept that CD mainly reflects brain dysfunctions. Research on this topic has shown controversial results, and while the classic assumption is that CD is not associated with structural changes in the brain [47], altered GM concentration in CD patients in the cerebellar flocculus, as well as in the basal ganglia, the thalamus and the motor cortex has been found [6]. Such differences from our findings may be explained by different methodological approaches: While the previously used whole-brain approaches have identified differences in various structures, regardless of their functional roles, we focused on areas associated with specific functions relevant for CD, such as neck movements, and therefore opted for a ROI approach, which grouped together voxels belonging to the same functional areas. Even though our choice may have been more conservative than other approaches, it suggests that CD-related brain dysfunctions are not linked to structural changes. Future research should further investigate this topic, for instance by applying multimodal imaging techniques or ultra-high field MR, which could reveal subtle structural changes undetectable with conventional MRI. A potential outlook of the current study is to corroborate the specificity of our findings by investigating patients with other forms of focal dystonia, for instance focal hand dystonia, where it is expected that only the connectivity of the hand representation areas within the PrG is selectively altered. In a study investigating network dysfunctions common to different forms of focal dystonia, the lateral motor cortex had abnormal connectivity with the intraparietal sulcus but not the cerebellum [48], suggesting that the functional connection we found between the medial motor cortex and the cerebellar vermis is part of the network specifically affected in cervical dystonia. Similarly, stratification of symptoms' type within CD,

such as tremor [49], and its effect on the cerebellar connectivity, should be investigated in a larger cohort of patients. We did not include patients with tremor due to its potential impact on image quality. Moreover, the correlation between symptoms' severity and brain functions, which showed only weak results in existing studies [34,50], should be further unraveled with a larger sample size.

In conclusion, our results point to an impairment in the communication of somato-specific cerebello-cortical networks related to head position and saccadic eye movements. This impairment might be the consequence of abnormal processing of proprioceptive input from the neck, which affects the functioning of the head neural integrator, and in turn generates abnormal head posture, as well as related compensatory eye movements.

Author contributions

Conception and design of the study: ER, YW. Data acquisition: CT, AE, CH, SS, AMB, CD, AM, BD, FB, MAB, PJ. Data analysis and interpretation: GAZ, CG, BB, MR, ER, YW. Writing of the first draft: GAZ, YW. Review and final approval: GAZ, CG, BB, MR, CT, AE, CH, SS, AMB, CD, AM, BD, FB, MAB, PJ, ER, YW.

Declaration of competing interest

None.

Acknowledgements

This work was supported by the Swiss National Science Foundation (P400PM_183958), AMADYS, Fondation Brou de Laurière, Merz-Pharma. This project was also supported by « Agence Nationale de la Recherche (ANR)» under the frame of the European Joint Programme on Rare Diseases (EJP RD, ANR-16-CE37-0003-03). The funding institutes had no role in the study design, data collection, analysis and interpretation of data, writing of the report, and the decision to submit the article for publication. The Authors would like to acknowledge the Swiss National Science Foundation (SNSF), the Paris Brain Institute, and the University Hospitals Pitié-Salpêtrière for the support. We would also like to thank all the participants of our study.

Appendix A. Supplementary data

Supplementary data to this article can be found online at https://doi.org/10.1016/j.parkreldis.2021.11.034.

References

[1] H.L. Geyer, S.B. Bressman, The diagnosis of dystonia, Lancet Neurol. 5 (9) (2006) 780–790.
[2] A. Quartarone, M. Hallett, Emerging concepts in the physiological basis of dystonia, Mov. Disord. 28 (7) (2013) 958–967.
[3] R.G. Burciu, C.W. Hess, S.A. Coombes, E. Ofori, P. Shukla, J.W. Chung, N. R. McFarland, A. Wagle Shukla, M.S. Okun, D.E. Vaillancourt, Functional activity of the sensorimotor cortex and cerebellum relates to cervical dystonia symptoms, Hum. Brain Mapp. 38 (9) (2017) 4563–4573.
[4] C.N. Prudente, E.J. Hess, H. Jinnah, Dystonia as a network disorder: what is the role of the cerebellum? Neuroscience 260 (2014) 23–35.
[5] P. Filip, C. Gallea, S. Lehéricy, E. Bertasi, T. Popa, R. Mareček, O.V. Lungu, T. Kašpárek, J. Vaníček, M. Bareš, Disruption in cerebellar and basal ganglia networks during a visuospatial task in cervical dystonia, Mov. Disord. 32 (5) (2017) 757–768.
[6] B. Draganski, C. Thun-Hohenstein, U. Bogdahn, J. Winkler, A. May, "Motor circuit" gray matter changes in idiopathic cervical dystonia, Neurology 61 (9) (2003) 1228–1231.
[7] B.D. Berman, J.M. Honce, E. Shelton, S.H. Sillau, L.M. Nagae, Isolated focal dystonia phenotypes are associated with distinct patterns of altered microstructure, Neuroimage: Clinical 19 (2018) 805–812.
[8] Y. Boillat, P.-L. Bazin, W. van der Zwaag, Whole-body somatotopic maps in the cerebellum revealed with 7T fMRI, Neuroimage 211 (2020) 116624.
[9] K. Friston, C. Frith, P. Liddle, R. Frackowiak, Functional connectivity: the principal-component analysis of large (PET) data sets, J. Cerebr. Blood Flow Metabol. 13 (1) (1993) 5–14.
[10] E. Consky, A. Basinski, L. Belle, R. Ranawaya, A. Lang, The Toronto Western spasmodic Torticollis rating scale (TWSTRS): assessment of validity and inter-rater reliability, Neurology 40 (suppl 1) (1990) 445.
[11] U. Braun, M.M. Plichta, C. Esslinger, C. Sauer, L. Haddad, O. Grimm, D. Mier, S. Mohnke, A. Heinz, S. Erk, Test–retest reliability of resting-state connectivity network characteristics using fMRI and graph theoretical measures, Neuroimage 59 (2) (2012) 1404–1412.
[12] Z. Li, A. Kadivar, J. Pluta, J. Dunlop, Z. Wang, Test–retest stability analysis of resting brain activity revealed by blood oxygen level-dependent functional MRI, J. Magn. Reson. Imag. 36 (2) (2012) 344–354.
[13] R.M. Birn, E.K. Molloy, R. Patriat, T. Parker, T.B. Meier, G.R. Kirk, V.A. Nair, M. E. Meyerand, V. Prabhakaran, The effect of scan length on the reliability of resting-state fMRI connectivity estimates, Neuroimage 83 (2013) 550–558.
[14] S.C. Strother, Evaluating fMRI preprocessing pipelines, IEEE Eng. Med. Biol. Mag. 25 (2) (2006) 27–41.
[15] M. Waltmann, O. O'Daly, A. Egerton, K. McMullen, V. Kumari, G.J. Barker, S. C. Williams, G. Modinos, Multi-echo fMRI, resting-state connectivity, and high psychometric schizotypy, Neuroimage: Clinical 21 (2019) 101603.
[16] F. Puledda, O. O'Daly, C. Schankin, D. Ffytche, S.C. Williams, P.J. Goadsby, Disrupted connectivity within visual, attentional and salience networks in the visual snow syndrome, Hum. Brain Mapp. 42 (7) (2021) 2032–2044.
[17] K. O'Gallagher, F. Puledda, O. O'Daly, M. Ryan, L. Dancy, P.J. Chowienczyk, F. Zelaya, P.J. Goadsby, A.M. Shah, Neuronal Nitric Oxide Synthase Regulates Regional Brain Perfusion in Healthy Humans, Cardiovascular research, 2021.
[18] D.J. Hohenschurz-Schmidt, G. Calcagnini, O. Dipasquale, J.B. Jackson, S. Medina, O. O'Daly, J. O'Muircheartaigh, A. de Lara Rubio, S.C. Williams, S.B. McMahon, Linking pain sensation to the autonomic nervous system: the role of the anterior cingulate and periaqueductal gray resting-state networks, Front. Neurosci. 14 (2020) 147.
[19] M. Jenkinson, C.F. Beckmann, T.E. Behrens, M.W. Woolrich, S.M. Smith, Fsl, Neuroimage 62 (2) (2012) 782–790.
[20] P. Kundu, S.J. Inati, J.W. Evans, W.-M. Luh, P.A. Bandettini, Differentiating BOLD and non-BOLD signals in fMRI time series using multi-echo EPI, Neuroimage 60 (3) (2012) 1759–1770.
[21] P. Kundu, V. Voon, P. Balchandani, M.V. Lombardo, B.A. Poser, P.A. Bandettini, Multi-echo fMRI: a review of applications in fMRI denoising and analysis of BOLD signals, Neuroimage 154 (2017) 59–80.
[22] O. Dipasquale, A. Sethi, M.M. Laganà, F. Baglio, G. Baselli, P. Kundu, N. A. Harrison, M. Cercignani, Comparing resting state fMRI de-noising approaches using multi-and single-echo acquisitions, PLoS One 12 (3) (2017), e0173289.
[23] J.D. Power, A. Mitra, T.O. Laumann, A.Z. Snyder, B.L. Schlaggar, S.E. Petersen, Methods to detect, characterize, and remove motion artifact in resting state fMRI, Neuroimage 84 (2014) 320–341.
[24] J.D. Power, K.A. Barnes, A.Z. Snyder, B.L. Schlaggar, S.E. Petersen, Spurious but systematic correlations in functional connectivity MRI networks arise from subject motion, Neuroimage 59 (3) (2012) 2142–2154.
[25] J.D. Power, M. Plitt, P. Kundu, P.A. Bandettini, A. Martin, Temporal interpolation alters motion in fMRI scans: magnitudes and consequences for artifact detection, PLoS One 12 (9) (2017), e0182939.
[26] L. Fan, H. Li, J. Zhuo, Y. Zhang, J. Wang, L. Chen, Z. Yang, C. Chu, S. Xie, A. R. Laird, The human brainnetome atlas: a new brain atlas based on connectional architecture, Cerebr. Cortex 26 (8) (2016) 3508–3526.
[27] S. Whitfield-Gabrieli, A. Nieto-Castanon, Conn: a functional connectivity toolbox for correlated and anticorrelated brain networks, Brain Connect. 2 (3) (2012) 125–141.
[28] Y. Behzadi, K. Restom, J. Liau, T.T. Liu, A component based noise correction method (CompCor) for BOLD and perfusion based fMRI, Neuroimage 37 (1) (2007) 90–101.
[29] J. Diedrichsen, A spatially unbiased atlas template of the human cerebellum, Neuroimage 33 (1) (2006) 127–138.
[30] M. Rebsamen, C. Rummel, M. Reyes, R. Wiest, R. McKinley, Direct cortical thickness estimation using deep learning-based anatomy segmentation and cortex parcellation, Hum. Brain Mapp. 41 (17) (2020) 4804–4814.
[31] Z. Li, C.N. Prudente, R. Stilla, K. Sathian, H.A. Jinnah, X. Hu, Alterations of resting-state fMRI measurements in individuals with cervical dystonia, Hum. Brain Mapp. 38 (8) (2017) 4098–4108.
[32] G. Battistella, P. Termsarasab, R.A. Ramdhani, S. Fuertinger, K. Simonyan, Isolated focal dystonia as a disorder of large-scale functional networks, Cerebr. Cortex 27 (2) (2015) bhv313.
[33] E. Sarasso, F. Agosta, N. Piramide, F. Bianchi, C. Butera, R. Gatti, S. Amadio, U. Del Carro, M. Filippi, Sensory trick phenomenon in cervical dystonia: a functional MRI study, J. Neurol. 267 (4) (2020) 1103–1115.
[34] S. Wei, C. Lu, X. Chen, L. Yang, J. Wei, W. Jiang, Y. Liu, H.H. Li, Y. Qin, Y. Lei, Abnormal regional homogeneity and its relationship with symptom severity in cervical dystonia: a rest state fMRI study, BMC Neurol. 21 (1) (2021) 1–8.
[35] M.C. Reddan, M.A. Lindquist, T.D. Wager, Effect size estimation in neuroimaging, JAMA psychiatry 74 (3) (2017) 207–208.
[36] K. Uehara, S. Furuya, H. Numazawa, K. Kita, T. Sakamoto, T. Hanakawa, Distinct roles of brain activity and somatotopic representation in pathophysiology of focal dystonia, Hum. Brain Mapp. 40 (6) (2019) 1738–1749.
[37] S. Butterworth, S. Francis, E. Kelly, F. McGlone, R. Bowtell, G.V. Sawle, Abnormal cortical sensory activation in dystonia: an fMRI study, Mov. Disord. 18 (6) (2003) 673–682.
[38] S. Tamburin, P. Manganotti, C.A. Marzi, A. Fiaschi, G. Zanette, Abnormal somatotopic arrangement of sensorimotor interactions in dystonic patients, Brain 125 (12) (2002) 2719–2730.

[39] R.S. Raike, C.E. Pizoli, C. Weisz, A.M. van den Maagdenberg, H. Jinnah, E.J. Hess, Limited regional cerebellar dysfunction induces focal dystonia in mice, Neurobiol. Dis. 49 (2013) 200–210.
[40] C.N. Prudente, R. Stilla, C.M. Buetefisch, S. Singh, E.J. Hess, X. Hu, K. Sathian, H. Jinnah, Neural substrates for head movements in humans: a functional magnetic resonance imaging study, J. Neurosci. 35 (24) (2015) 9163–9172.
[41] J. Voogd, C.K. Schraa-Tam, J.N. van der Geest, C.I. De Zeeuw, Visuomotor cerebellum in human and nonhuman primates, Cerebellum 11 (2) (2012) 392–410.
[42] A. Mahajan, P. Gupta, J. Jacobs, L. Marsili, A. Sturchio, H. Jinnah, A.J. Espay, A. G. Shaikh, Impaired Saccade Adaptation in Tremor-Dominant Cervical Dystonia—Evidence for Maladaptive Cerebellum, The Cerebellum, 2020, pp. 1–9.
[43] A. Hirsig, C. Barbey, M.W. Schüpbach, P. Bargiotas, Oculomotor functions in focal dystonias: a systematic review, Acta Neurol. Scand. 141 (5) (2020) 359–367.
[44] M. Argyelan, M. Carbon, M. Niethammer, A.M. Uluğ, H.U. Voss, S.B. Bressman, V. Dhawan, D. Eidelberg, Cerebellothalamocortical connectivity regulates penetrance in dystonia, J. Neurosci. 29 (31) (2009) 9740–9747.
[45] A.G. Shaikh, D.S. Zee, J.D. Crawford, H.A. Jinnah, Cervical dystonia: a neural integrator disorder, Brain 139 (10) (2016) 2590–2599.
[46] T. Popa, C. Hubsch, P. James, A. Richard, M. Russo, S. Pradeep, S. Krishan, E. Roze, S. Meunier, A. Kishore, Abnormal cerebellar processing of the neck proprioceptive information drives dysfunctions in cervical dystonia, Sci. Rep. 8 (1) (2018) 1–10.
[47] R.-M. Gracien, F. Petrov, P. Hok, A. van Wijnen, M. Maiworm, A. Seiler, R. Deichmann, S. Baudrexel, Multimodal quantitative MRI reveals no evidence for tissue pathology in idiopathic cervical dystonia, Front. Neurol. 10 (2019) 914.
[48] S.A. Norris, A.E. Morris, M.C. Campbell, M. Karimi, B. Adeyemo, R.C. Paniello, A. Z. Snyder, S.E. Petersen, J.W. Mink, J.S. Perlmutter, Regional, not global, functional connectivity contributes to isolated focal dystonia, Neurology 95 (16) (2020) e2246–e2258.
[49] D. Martino, G. Bonassi, G. Lagravinese, E. Pelosin, G. Abbruzzese, L. Avanzino, Defective human motion perception in cervical dystonia correlates with coexisting tremor, Mov. Disord. 35 (6) (2020) 1067–1071.
[50] D. Kroneberg, P. Plettig, G.H. Schneider, A.A. Kühn, Motor cortical plasticity relates to symptom severity and clinical benefit from deep brain stimulation in cervical dystonia, Neuromodulation: Technol. Neural Interfac. 21 (8) (2018) 735–740.